Claudin-7 Regulates EpCAM-Mediated Functions in Tumor Progression

Tobias Nübel,[1] Julia Preobraschenski,[1] Hüseyin Tuncay,[1] Tobias Weiss,[1] Sebastian Kuhn,[1] Markus Ladwein,[1] Lutz Langbein,[2] and Margot Zöller[1,3,4]

Departments of [1]Tumor Progression and Immune Defense and [2]Cell Biology, German Cancer Research Center; [3]Department of Tumor Cell Biology, University Hospital of Surgery, Heidelberg, Germany; and [4]Department of Applied Genetics, University of Karlsruhe, Karlsruhe, Germany

Abstract

EpCAM has been described as a therapeutically relevant tumor marker. We noted an interaction between EpCAM and the tight junction protein claudin-7 and here explored the nature of this interaction and its effect on EpCAM-mediated functions. The interaction between EpCAM and claudin-7 was defined in HEK293 cells transfected with rat claudin-7 and EpCAM cDNA. Deletions of the epidermal growth factor–like and the thyroglobin repeat domains of EpCAM or the cytoplasmic domain of EpCAM or claudin-7 did not prevent the EpCAM-claudin-7 association. A chimeric EpCAM molecule with an exchange of the cytoplasmic and transmembrane domains and an EpCAM molecule with point mutations in an AxxxG motif in the transmembrane region do not associate with claudin-7. HEK cells and the rat pancreatic tumor line BSp73AS, transfected with (mutated) EpCAM and claudin-7 cDNA, revealed that the association of both molecules severely alters the functional activity of EpCAM. Claudin-7–associated EpCAM is recruited into tetraspanin-enriched membrane microdomains (TEM). The TEM-located claudin-7-EpCAM complex supports proliferation accompanied by sustained extracellular signal–regulated kinase-1/2 phosphorylation, up-regulation of antiapoptotic proteins, and drug resistance, but not EpCAM-mediated cell-cell adhesion. Enhanced motility may be supported by colocalization of claudin-7 with actin bundles, which is only seen in EpCAM-claudin-7–expressing cells. The EpCAM-claudin-7 complex strongly promotes tumorigenicity, accelerates tumor growth, and supports ascites production and thymic metastasis formation. High expression of the tumor marker EpCAM is frequently associated with poor prognosis, which could well rely on the EpCAM-claudin-7 association that prohibits EpCAM-mediated cell-cell adhesion but promotes migration, proliferation, apoptosis resistance, and tumorigenicity. (Mol Cancer Res 2009;7(3):285–99)

Introduction

The epithelial cell adhesion molecule EpCAM (EpC) is expressed on many epithelia (1, 2) and its expression is frequently increased in nearly all carcinomas as well as myelomas (1-12). Depending on the tumor type, high EpC expression correlates with tumor grading and/or tumor-node-metastasis staging and/or decreased overall and poor disease-free survival (4, 5, 13, 14). EpC has also been described as a cancer-initiating cell marker of mammary, colorectal, and pancreatic cancers (15-19).

EpC is a type I transmembrane molecule with an epidermal growth factor (EGF)–like domain, followed by a thyroglobin repeat (TG) domain (20), a cysteine-poor region, a transmembrane, and a short cytoplasmic domain (21). Both the EGF-like domain and the TG domain form a globular structure and are required for the homophilic cell-cell adhesion of EpC. The EGF-like domain is required for the reciprocal and the TG domain for the lateral interaction of EpC molecules (22). Both domains are required for the anchoring of actin microfilaments at the cell membrane via α-actinin, a process regulated by the cytoplasmic tail of EpC (22). On the other hand, and in line with cell-cell adhesion preventing metastasis formation (23), EpC has been reported to abrogate E-cadherin–mediated cell-cell adhesion by disrupting the link between α-catenin and F-actin (3, 24), which points to a possible involvement of EpC in tumor progression (25). In addition, EpC can support cell motility and become involved in signal transduction and cell proliferation via up-regulation of cyclin A and cyclin E synthesis (26-28). The phenotype of EpC transgenic mice with high-level bcl-2 and Ki67 expression supports a role of EpC in mitogenic signaling (29). Finally, EpC also induces up-regulation of the proto-oncogene *c-myc* (30), where EpC cross-linking triggers, together with tumor necrosis factor–converting enzyme and presenilin 2 NH_2-terminal fragment, signals that cleave an intracellular peptide of EpC, EpIC, which forms a complex with β-catenin and Lef-1; locates to the nucleus; and, by binding to Lef consensus sites, initiates *c-myc* transcription (31).

Received 4/22/08; revised 9/15/08; accepted 10/15/08; published OnlineFirst 3/10/09.

Grant support: Mildred-Scheel-Stiftung für Krebsforschung (M. Zöller) and Tumorzentrum Heidelberg/Mannheim (M. Zöller).

The costs of publication of this article were defrayed in part by the payment of page charges. This article must therefore be hereby marked *advertisement* in accordance with 18 U.S.C. Section 1734 solely to indicate this fact.

Note: Supplementary data for this article are available at Molecular Cancer Research Online (http://mcr.aacrjournals.org/).

Current address for M. Ladwein: Cytoskeleton Dynamics Group, HGF Centre for Infection Research, Braunschweig, Germany.

Requests for reprints: Margot Zöller, Department of Tumor Cell Biology, University Hospital of Surgery, Im Neuenheimer Feld 365, D-69120 Heidelberg, Germany. Phone: 49-6221-565146; Fax: 49-6221-565199. E-mail: m.zoeller@dkfz.de

doi:10.1158/1541-7786.MCR-08-0200

Our own studies have been concerned on the importance of EpC expression in tumor progression and in tumor progression–related functional activities. EpC overexpression in a nonmetastasizing rat pancreatic adenocarcinoma line (BSp73AS) does not suffice to promote metastasis formation, but it provides a growth-promoting stimulus *in vivo* (32). In the metastatic BSp73ASML subline, EpC is associated with claudin-7 (cld-7), CD44v, several integrins, and the tetraspanin D6.1A (33-35), where only the EpC-cld-7 association is based on a direct protein-protein interaction (14, 34). Tetraspanins are located in glycolipid-enriched membrane microdomains (14, 34), called tetraspanin-enriched membrane microdomains (TEM), which serve as a signaling platform (36, 37). According to its association with tetraspanins, the EpC-cld-7 complex is supposed to be TEM located. In fact, there is evidence for cooperative activity of the EpC-cld-7-CD44v-tetraspanin complex (14, 33, 34). Matrix adhesion and cluster formation of tumor cells expressing the complex, but not the individual molecules, is reduced after partial cholesterol depletion, which destroys TEM. In human colorectal cancer, coexpression of EpC, cld-7, CO-029, and CD44v6 inversely correlates with the disease-free survival, and colorectal cancer lines that express the complex display a higher degree of apoptosis resistance than lines devoid of any one of the four

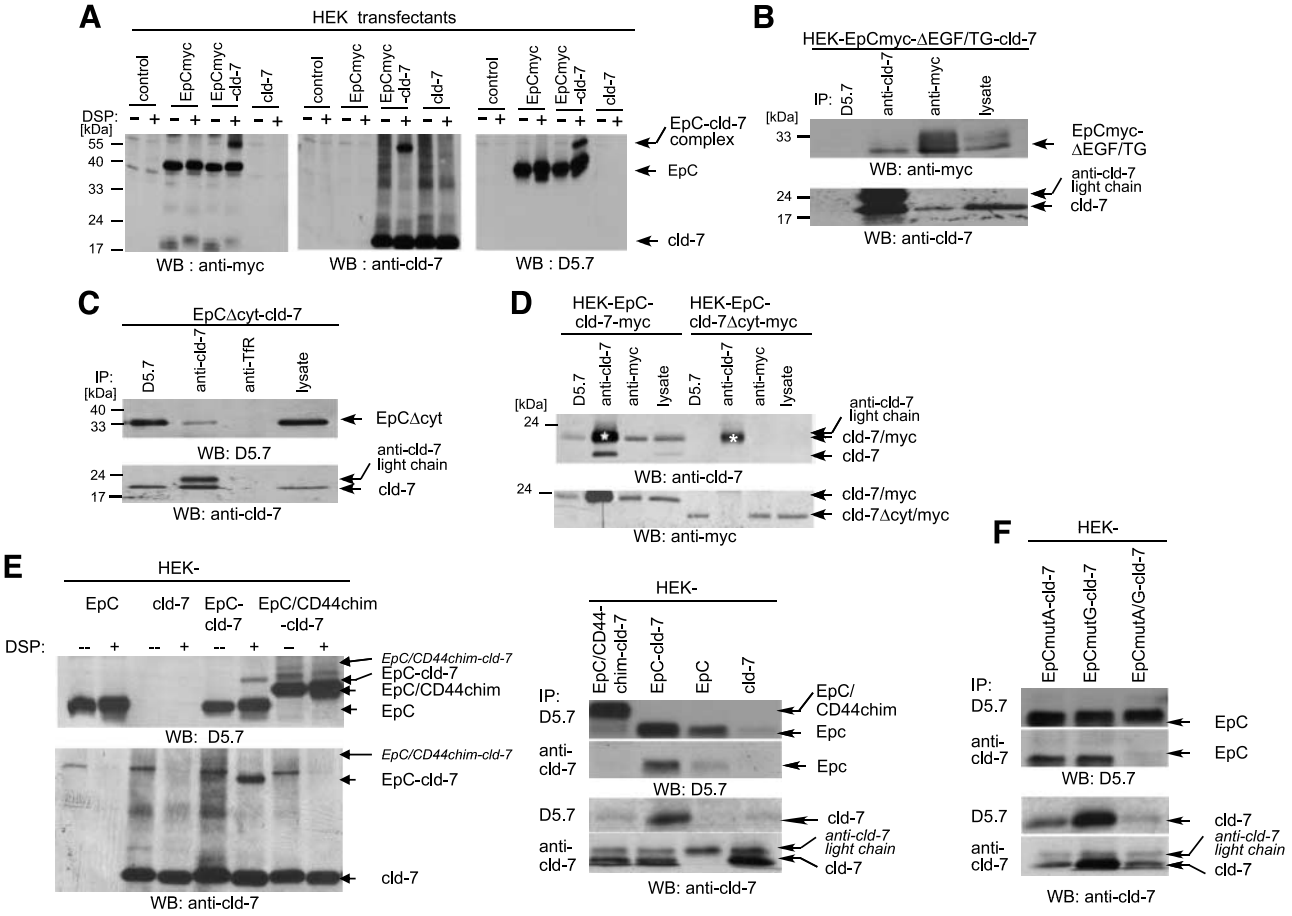

FIGURE 1. Transmembrane association of EpC with cld-7. **A.** HEK cells were transfected with *EpCmyc, cld-7*, or *EpCmyc* plus *cld-7* cDNA. Where indicated, cells were treated with the membrane-permeable chemical cross-linker dithio-bis-succinimidylproprionate (*DSP*). After lysis, SDS-PAGE, and transfer, samples were blotted with anti-myc, anti–cld-7, or D5.7. EpC, cld-7, and the EpC-cld-7 complex are indicated. **B.** HEK cells were transfected with *myc*-tagged *EpCΔEGF/TG* cDNA and *cld-7* cDNA. After lysis, immunoprecipitation with D5.7, anti-myc, and anti–cld-7, SDS-PAGE, and transfer, samples were blotted with anti-myc and anti–cld-7. Anti-cld-7 coprecipitates EpCmyc-ΔEGF/TG [Western blot (*WB*): anti-myc] and anti-myc coimmunoprecipitates cld-7 (Western blot: anti–cld-7). **C.** HEK cells were transfected with *EpCΔcyt* cDNA and *cld-7* cDNA. After lysis, immunoprecipitation with anti-EpC, anti–cld-7, and anti–transferrin receptor (*TfR*; negative control), SDS-PAGE, and transfer, samples were blotted with D5.7 and anti–cld-7. D5.7 coimmunoprecipitates cld-7 (Western blot: cld-7) and anti–cld-7 coimmunoprecipitates EpCΔcyt. **D.** HEK cells were transfected with *EpC* cDNA and *myc*-tagged *cld-7Δcyt* cDNA. After lysis, immunoprecipitation with anti-EpC, anti–cld-7, and anti-myc, SDS-PAGE, and transfer, samples were blotted with anti-myc and anti–cld-7. D5.7 coimmunoprecipitates cld-7/myc and cld-7Δcyt/myc, which is only visible in the Western blot with anti-myc because anti–cld-7 does not recognize cld-7Δcyt. Anti-cld-7 precipitates only cld-7/myc, but not anti–cld-7Δcyt/myc. (The band visible in the Western blot with anti–cld-7, marked by a white star, is slightly higher and corresponds to the anti–cld-7 light chain, also visible in **B** and **D**.) Accordingly, the cld-7Δcyt/myc precipitate is only visible in the Western blot with anti-myc. **E.** HEK cells were transfected with *cld-7* cDNA and chimeric *EpC/CD44* cDNA, where the cDNA of the transmembrane and the cytoplasmic domain of EpC was replaced by the corresponding CD44 cDNA. Where indicated, cells were treated with the membrane-permeable cross-linker dithio-bis-succinimidylproprionate. After lysis, SDS-PAGE, and transfer, samples were blotted with D5.7 and anti–cld-7. EpC/CD44chim did not associate with cld-7 (expected band size is indicated in italics. **F.** Amino acids A279 and G282 in the transmembrane region of EpC, which potentially could interact with neighboring proteins, have been exchanged. After lysis, immunoprecipitation with D5.7 and anti–cld-7, SDS-PAGE, and transfer, samples were blotted with D5.7 and anti–cld-7. EpC-mutA/G does not coimmunoprecipitate with cld-7.

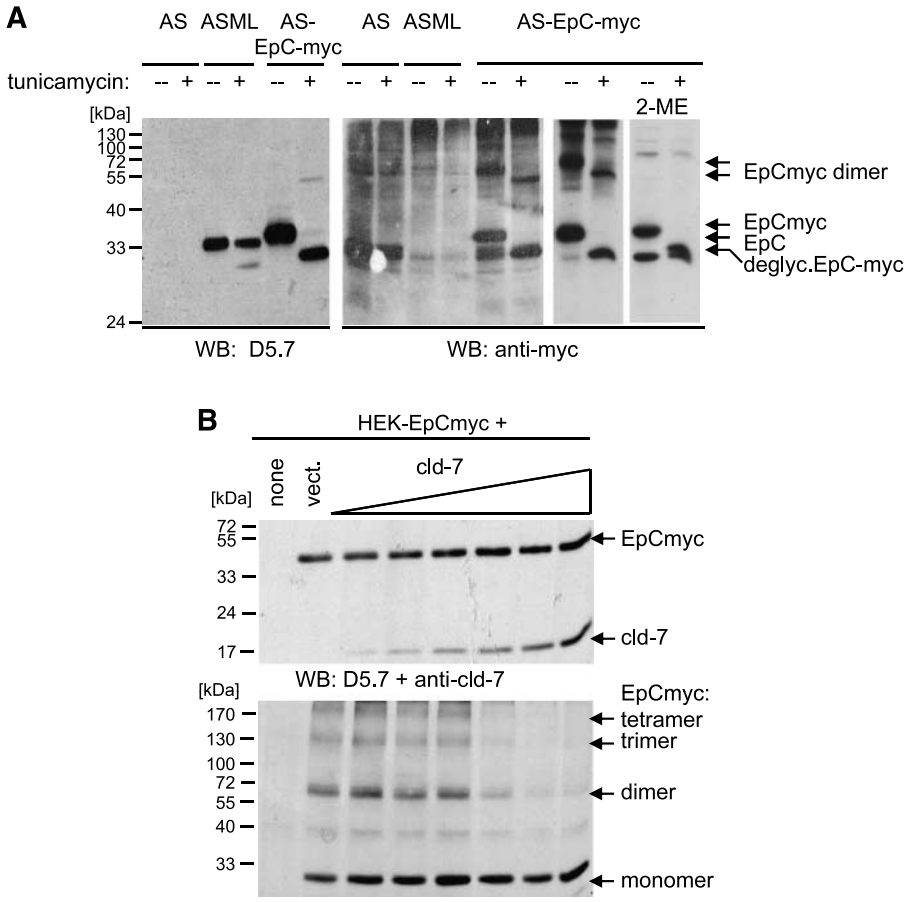

FIGURE 2. Cld-7 interferes with EpC oligomerization. **A.** AS, ASML, and *EpCmyc* cDNA–transfected AS cells were treated with tunicamycin or 2-mercaptoethanol (*2-ME*), lysed, and separated by SDS-PAGE. After transfer, samples were blotted with anti-myc and D5.7. EpC and deglycosylated EpC are detected in ASML and AS-EpCmyc lysates with D5.7 and anti-myc. EpC oligomers are only detected with anti-myc and only in AS-EpCmyc lysates. Oligomers were not detected after 2-mercaptoethanol treatment. **B.** HEK-EpCmyc cells were transfected with increasing amounts of *cld-7* cDNA. After SDS-PAGE and transfer, samples were blotted with D5.7, anti–cld-7, and anti-myc. Monomeric EpC is detected in all blots, and oligomeric EpC only in the anti-myc blot. The formation of oligomeric EpC correlates inversely with cld-7 expression.

molecules. Down-modulation of EpC or cld-7 expression by small interfering RNA is accompanied by a loss in apoptosis resistance (14).

To proceed toward unraveling the mechanisms that account for EpC functioning as a tumor marker, we defined the mode of the EpC-cld-7 association. Using EpC/mutated EpC plus cld-7 cDNA transfected tumor lines, we provide evidence that neither EpC nor cld-7, but the EpC-cld-7 complex promotes tumor growth and progression.

Results

The Transmembrane Domain of EpC Is Decisive for Complex Formation

Coimmunoprecipitation of EpC and cld-7 is only observed with a membrane-permeable cross-linker (34). The finding suggests that the extracellular domain may not be involved. To control our hypothesis that the association of EpC with cld-7 (14, 34) may play a decisive role in EpC-mediated functions, we first defined the interaction site between EpC and cld-7. HEK cells were transfected with deletion mutants of *EpC* and *cld-7* cDNA, which were tagged with *myc* as long as the deletion included the antibody binding site. Because T-antigen–transformed HEK cells express EpC,[5] nontransformed HEK cells were used for transfection throughout. Schemes of the mutated cDNAs and protein expression levels are shown in Supplementary Fig. S1. The myc tag on EpC does not interfere with EpC expression or with the EpC-cld-7 association (Fig. 1A). As expected, the EpC-cld-7 association is not perturbed when both the EGF and TG domains of EpC are deleted (Fig. 1B). The EpC-cld-7 association is also preserved when the cytoplasmic tail of EpC or cld-7 is deleted. Anti-EpC and anti-myc coprecipitate EpCΔcyt and cld-7 (Fig. 1C); anti-EpC, anti–cld-7, and anti-myc precipitate cld-7-myc. However, anti–cld-7 does not recognize cld-7Δcyt. Therefore, anti-EpC, anti–cld-7 (control), and anti-myc precipitates were blotted with anti-myc. Both anti-EpC and anti-myc precipitated cld-7Δcyt-myc (Fig. 1D). Therefore, the cytoplasmic tail cannot be the interaction site. There remains the transmembrane domain of EpC as a possible association site. In fact, when HEK cells were transfected with an EpC/CD44 chimeric cDNA, with the transmembrane and cytoplasmic domains of EpC being replaced by the corresponding *CD44* cDNA, the chimeric molecule is expressed at the cell surface but does not associate with cld-7. Thus, after chemical cross-linking, EpC and EpC-cld-7 were detected with anti-EpC in HEK-EpC-cld-7 lysates. However, in HEK-EpC/CD44chim-cld-7 lysates, only EpC/CD44chim, but not EpC-CD44chim-cld-7, was detected. Accordingly, blotting with anti–cld-7 revealed cld-7, but not EpC/CD44chim-cld-7. Furthermore, when HEK-EpC/CD44chim-cld-7 lysate was

[5] O. Gires, personal communication.

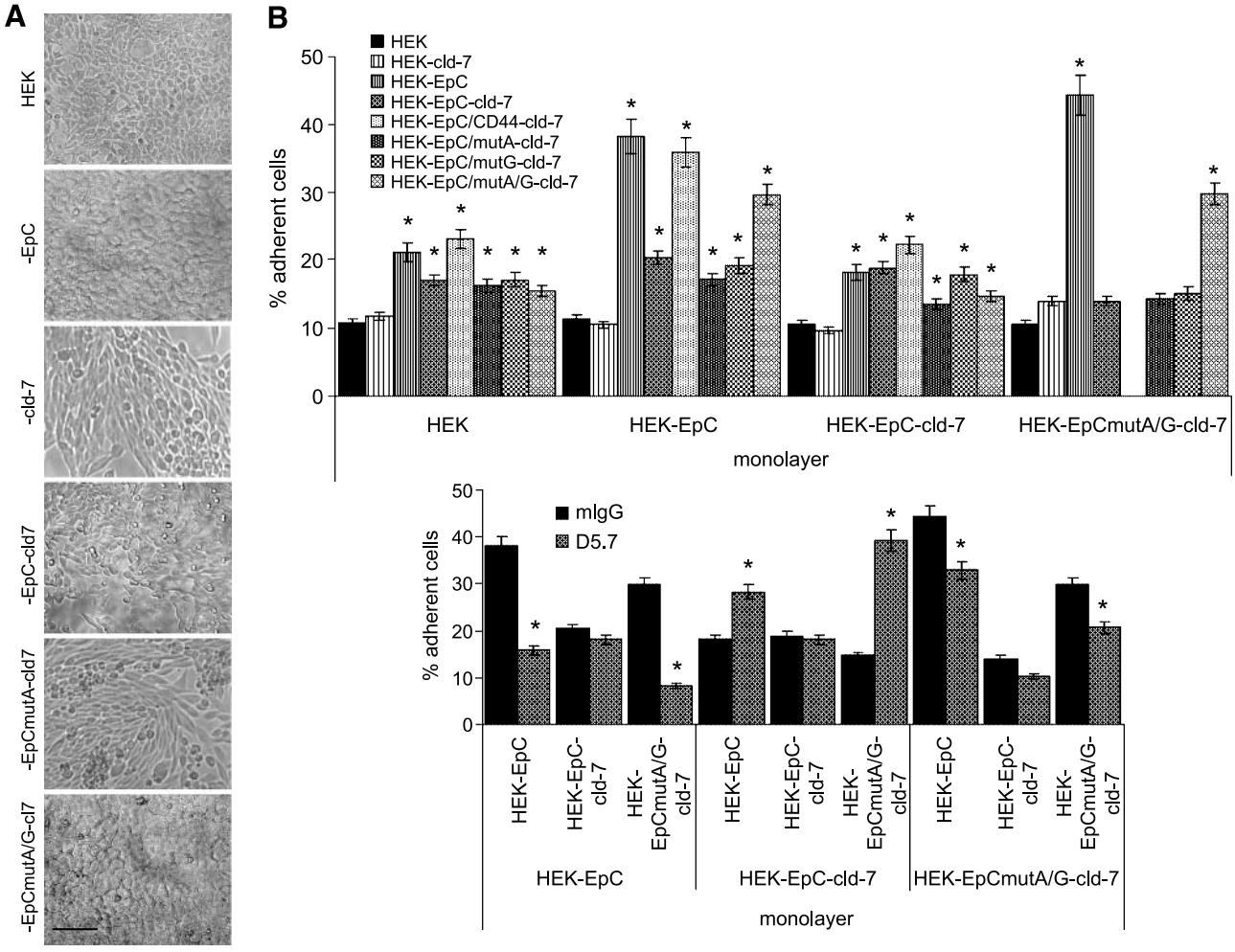

FIGURE 3. Cld-7–associated EpC does not mediate homophilic cell-cell adhesion. **A.** *In vitro* growth of HEK, HEK-EpC, HEK-EpC-cld-7, HEK-EpCmutA-cld-7, and HEK-EpCmutA/G-cld-7. Cells were seeded on plastic. Pictures were taken with an inverted microscope 24 h after seeding. Bar, 0.5 μm. **B.** HEK, HEK-cld-7, HEK-EpC, HEK-EpC-cld-7, HEK-EpC/CD44-cld-7, HEK-EpCmutA-cld-7, HEK-EpCmutG-cld-7, and HEK-EpCmutA/G-cld-7 cells were labeled with carboxyfluorescein diacetate succinimidyl ester (*CSFE*) and seeded on the indicated monolayers in flat-bottomed 96-well plates. Where indicated, the medium contained 10 μg/mL D5.7. After 2 h at 37°C, plates were washed. Adherent, carboxyfluorescein diacetate succinimidyl ester–labeled cells were quantified in an ELISA reader at 353 nm. Columns, mean percentages of adherent cells, as compared with total input of labeled cells, from triplicate experiments; bars, SD. *, significant differences in adhesion of HEK versus transfected HEK cells.

precipitated with anti-EpC, the precipitate did not contain cld-7, and anti–cld-7 precipitates did not contain EpC (Fig. 1E). To define more precisely the interaction site between EpC and cld-7, the two small amino acids A279 and G282 in the AxxxG motif (38) of the transmembrane domain of EpC were exchanged. Mutating A279 or G282 to I results in a minor reduction in EpC-cld-7 coimmunoprecipitation. Exchange of both amino acids has no effect on EpC expression. However, the mutated EpC does not coimmunoprecipitate with cld-7 and vice versa (Fig. 1F).

Thus, the association between EpC and cld-7 essentially relies on a defined amino acid motif in the transmembrane domain. The generation of HEK cells that express both EpC and cld-7 at high level, where EpC and cld-7 do or do not associate depending on the exchange of two amino acids, provided an optimal means to differentiate between EpC, cld-7, and EpC-cld-7 complex–mediated functions.

Cld-7 Prohibits EpC Oligomerization

Homophilic cell-cell adhesion is the most well-defined function of EpC (3). Thus, we asked whether EpC-associated cld-7 hampers EpC-mediated cell-cell adhesion. Because homophilic cell-cell adhesion of EpC requires lateral tetramer formation (3), the direct interaction of cld-7 with EpC could well interfere with EpC oligomerization.

EpC oligomerization was first evaluated in ASML cells and in AS cells transfected with myc-tagged EpC. Myc-tagged EpC cDNA was chosen because homophilic adhesion could occupy the D5.7 antibody binding site. This obviously is the case. EpC oligomers were only detected in AS-EpC-myc lysates after SDS-PAGE separation under nonreducing conditions when blotted with anti-myc but not with anti-EpC. EpC oligomers were also not detected in ASML lysates. As revealed by tunicamycin treatment (5 μg/mL, overnight), N-glycosylation is not required for oligomerization. Instead, a conformational

change due to disrupting disulfide bonds by 2-mercaptoethanol treatment (50 mmol/L, 30 minutes) prohibits oligomerization in AS-EpC-myc cells, which implies appropriate folding of EpC as a prerequisite for oligomerization (Fig. 2A). The association with cld-7 also interferes with EpC oligomerization. When EpC cDNA–transfected HEK cells were cotransfected with increasing amounts of cld-7 cDNA, the presence of dimers and tetramers inversely correlates with cld-7 expression. It should be noted that the band for monomeric EpC does not become more intense concomitantly with the loss of oligomeric EpC (Fig. 2B). Thus, only a minor portion of EpC will be in the oligomeric state. In addition, we failed to detect EpC oligomers in two-dimensional native polyacrylamide gels (data not shown), which may be a consequence of only low amounts of oligomerized EpC.

Taken together, there is compelling evidence that cld-7 interferes with oligomerization, which could affect EpC-mediated cell-cell adhesion.

EpC-Associated Cld-7 Influences Cell-Cell Adhesion and Motility

The hypothesis that EpC-associated cld-7 interferes with homophilic EpC-mediated cell-cell adhesion was supported by the different morphology of HEK-EpC versus HEK-EpC-cld-7 cells. HEK cells show an epitheloid morphology and are in loose contact, mostly via cell protrusions. The intercellular space appears much smaller in HEK-EpC cells, whereas HEK-EpC-cld-7 and HEK-EpCmutA-cld-7 cells have a fibroid morphology and grow rather dispersed. HEK cells transfected with *EpCmutA/G* plus *cld-7* cDNA display a growth pattern similar to HEK-EpC cells (Fig. 3A). Although less pronounced in AS than in HEK cells, similar differences in the growth pattern were seen with AS, AS-EpC, AS-cld-7, and AS-EpC-cld-7 cells, as also shown by phalloidin-FITC staining (Supplementary Fig. S2A). The finding indicates that only EpC by itself might support tight cell-cell adhesion.

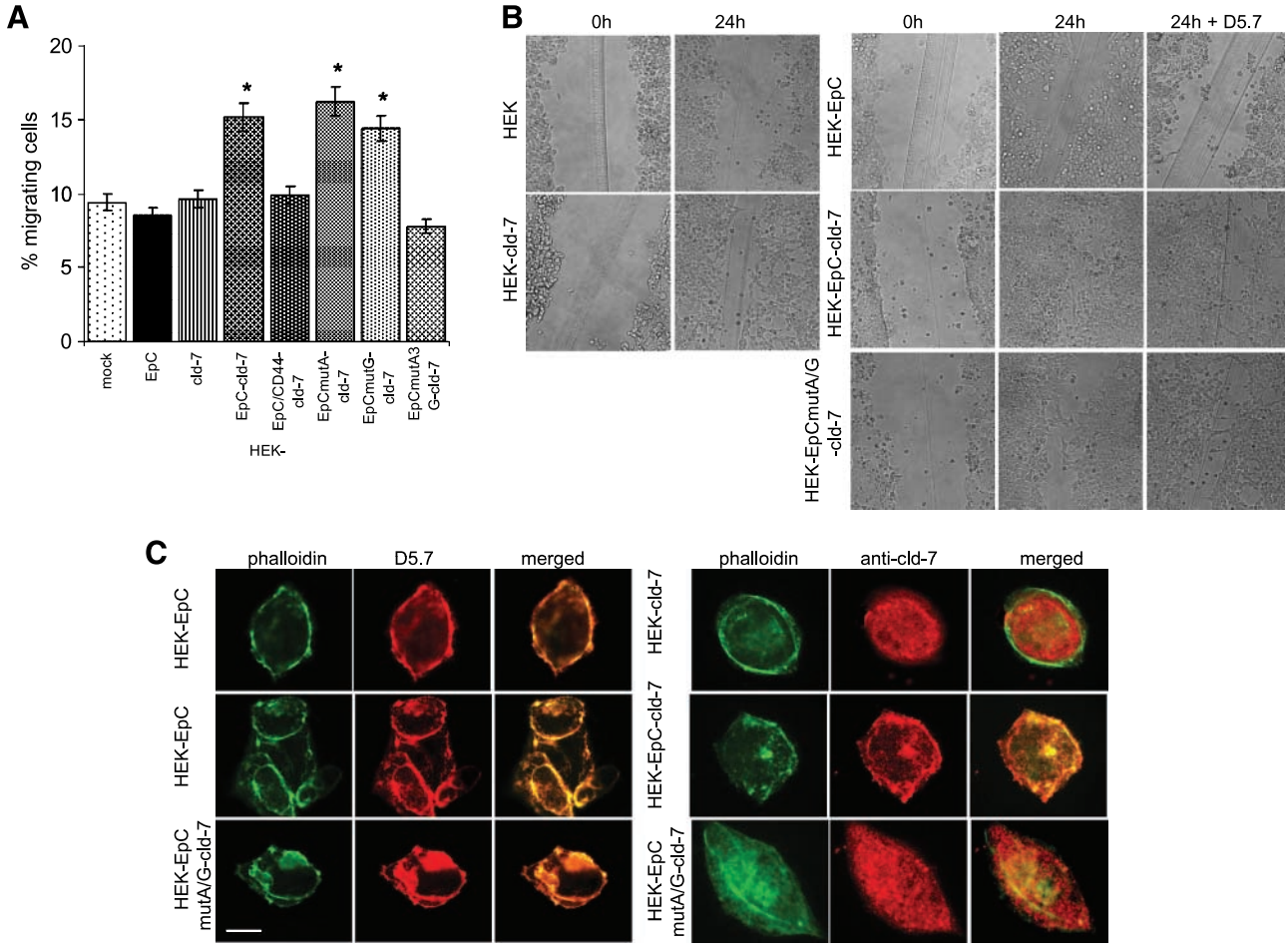

FIGURE 4. Cld-7–associated EpC promotes cell motility. **A.** Cells described in Fig. 3 were suspended in serum-free medium and seeded in the upper chamber of transwell plates. The lower chamber contained medium/10% FCS. Chambers were incubated for 24 h at 37°C. Cells on the lower site of the membrane were stained with crystal violet. The color reaction was measured in an ELISA reader. Columns, mean percentage of migrating cells from triplicate experiments; bars, SD. *, significant differences in migration as compared with HEK cells. **B.** Cells described above were seeded in 3-cm-diameter Petri dishes. Subconfluent cultures were wounded with a microtip. After wounding, D5.7 (10 μg/mL) was added where indicated. Wound healing was documented immediately and 24 h after wounding. It should be noted that HEK cells retracted from the scratch immediately after wounding. Bar, 0.3 μm. **C.** Cells were seeded on glass cover slides and stained with phalloidin-FITC and D5.7 or anti–cld-7 and Texas red–labeled secondary antibody. Single fluorescence images and digitally merged overlays are shown. Bar, 5 μm.

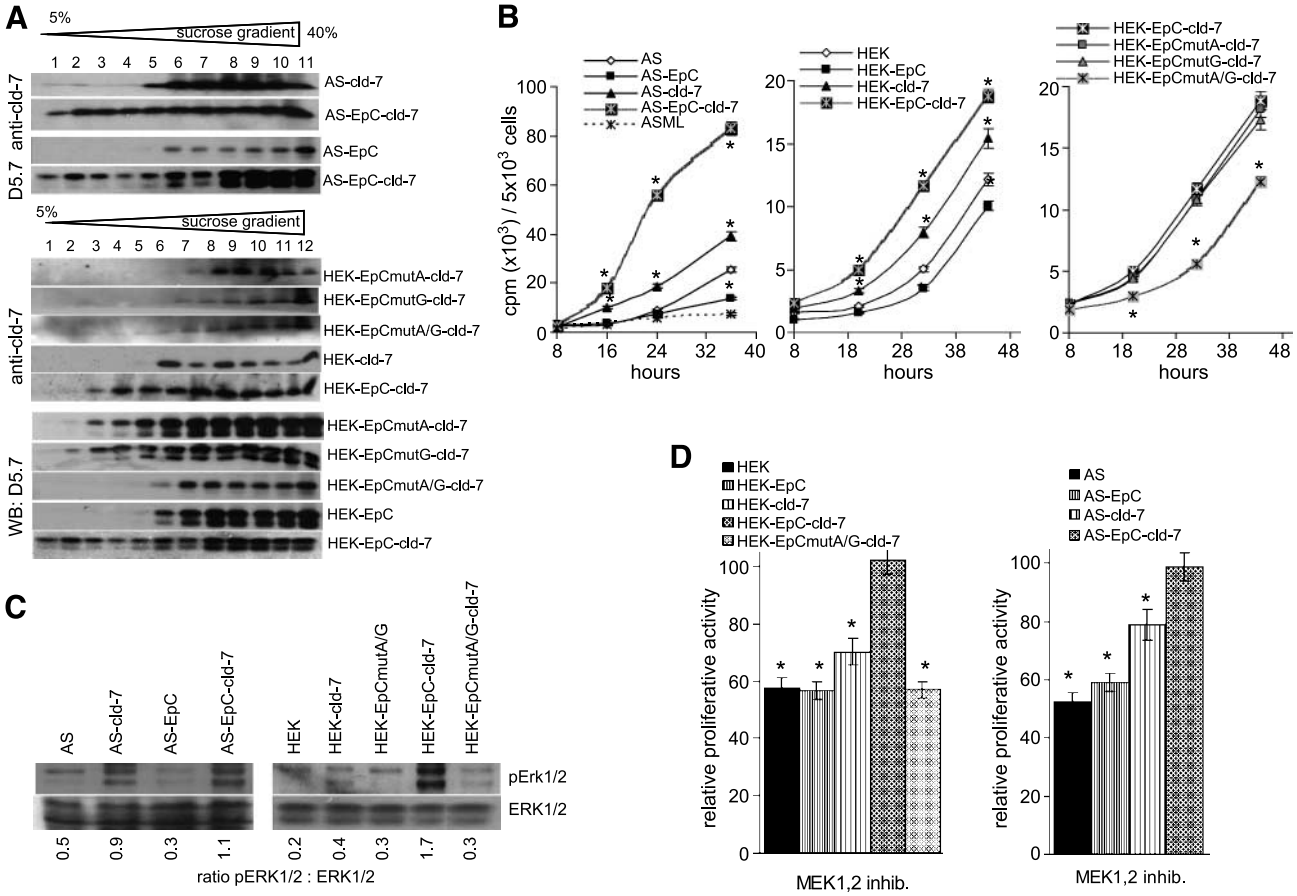

Figure 5. The effect of cld-7–associated EpC on tumor cell proliferation. **A.** Lysates of AS-EpC, AS-cld-7, and AS-EpC-cld-7 cells and of HEK-EpC, HEK-cld-7, HEK-EpC-cld-7, HEK-EpCmutA/G-cld-7, HEK-EpCmutA-cld-7, and HEK-EpCmutG-cld-7 cells were separated by sucrose density gradient centrifugation. Fractions were collected, separated by SDS-PAGE, transferred, and blotted with D5.7 and anti–cld-7. **B.** ASML, AS, AS-EpC, AS-cld-7, AS-EpC-cld-7, HEK, HEK-EpC, HEK-cld-7, HEK-EpC-cld-7, HEK-EpCmutA-cld-7, HEK-EpCmutG-cld-7, and HEK-EpCmutA/G-cld-7 cells (5×10^3) were seeded in flat-bottomed 96-well plates and cultured for up to 36 or 48 h at 37°C. [^{3}H]Thymidine was added during the last 8 h of culture. Cells were harvested and [^{3}H]thymidine incorporation was evaluated in a beta-counter. Points, mean counts per minute (*cpm*) per 5×10^3 cells from triplicate experiments; bars, SD. *, significant differences as compared with AS or HEK or HEK-EpC-cld-7. **C.** Cells described in **B** were lysed and lysates were separated by SDS-PAGE. Transferred proteins were blotted with anti-ERK1/2 and anti-pERK1/2. **D.** Cells described in **B** were cultured for 48 h in the presence of a MEK1/2 inhibitor. [^{3}H]Thymidine was added during the last 8 h of culture. The relative proliferative activity as compared with cells cultured in the absence of an inhibitor is shown. *, significant differences.

HEK cells transfected with EpC and/or cld-7 were incubated in Ca^{2+}-free medium on a rocking platform for 1 hour. HEK-EpC and HEK-EpCmutA/G-cld-7 cells, but not HEK-cld-7 and HEK-EpC-cld-7 cells, form large aggregates. When cells were rested for 12 hours, HEK-EpC and HEK-EpCmutA/G-cld-7 aggregates remained stable with only a few cells settling on the plastic. HEK and HEK-cld-7 cells form small aggregates that settle on top of the mostly plastic-adherent cells. HEK-EpC-cld-7 cells, different from HEK cells and all other transfectants, readily spread on plastic within 12 hours. However, it should be mentioned that this phenomenon was hardly observed after prolonged culture (see Fig. 3A) because after a period of 3 to 4 days (as shown in Fig. 3A), nontransfected and transfected HEK cells have a strong tendency to grow in colonies, wherein part of the cells lift up. Gentle shaking in the presence of the EpC-specific antibody D5.7 has no effect on the aggregation of HEK-EpC or HEK-EpCmutA/G-cld-7 cells but supports the aggregation of HEK-EpC-cld-7 cells, which possibly could be due to cross-linking of cells via the antibody. The fact that D5.7 also does not block HEK-EpC or HEK-EpCmutA/G-cld-7 aggregation supports our interpretation that D5.7 may not occupy the site of homophilic EpCAM-mediated cell adhesion. After a resting period of 12 hours, the small HEK-EpC-cld-7 aggregates are mostly dissolved (Supplementary Fig. S2B). The same observations account for AS-EpC and AS-EpC-cld-7 cells, with only AS-EpC forming small aggregates (data not shown).

Cell-cell adhesion was also evaluated by seeding carboxyfluorescein diacetate succinimidyl ester–labeled, untransfected and transfected HEK or AS cells on the respective monolayers. A significantly higher percentage of HEK-EpC cells adhere to HEK-EpC than to HEK cells. On the contrary, HEK-EpC-cld-7 cells display only slightly increased adhesion to HEK-EpC as compared with HEK cells. Yet, when the association between EpC and cld-7 is disturbed by deletion of the transmembrane and the cytoplasmic tail (HEK-EpC/CD44chim-cld-7) or the A

plus G mutation in the transmembrane region (HEK-EpCmutA/G-cld-7), cell-cell adhesion is in the same range as that in HEK-EpC cells. The EpC-specific antibody D5.7 inhibits adhesion of HEK-EpC and HEK-EpCmutA/G-cld-7 to a monoloayer of HEK-EpC or HEK-EpCmutA/G-cld-7 cells. On the contrary, D5.7 augments adhesion of these cells to HEK-EpC-cld-7 cells (Fig. 3B). Cell-cell adhesion between AS-EpC-cld-7 cells is also in the same range as that between AS cells,

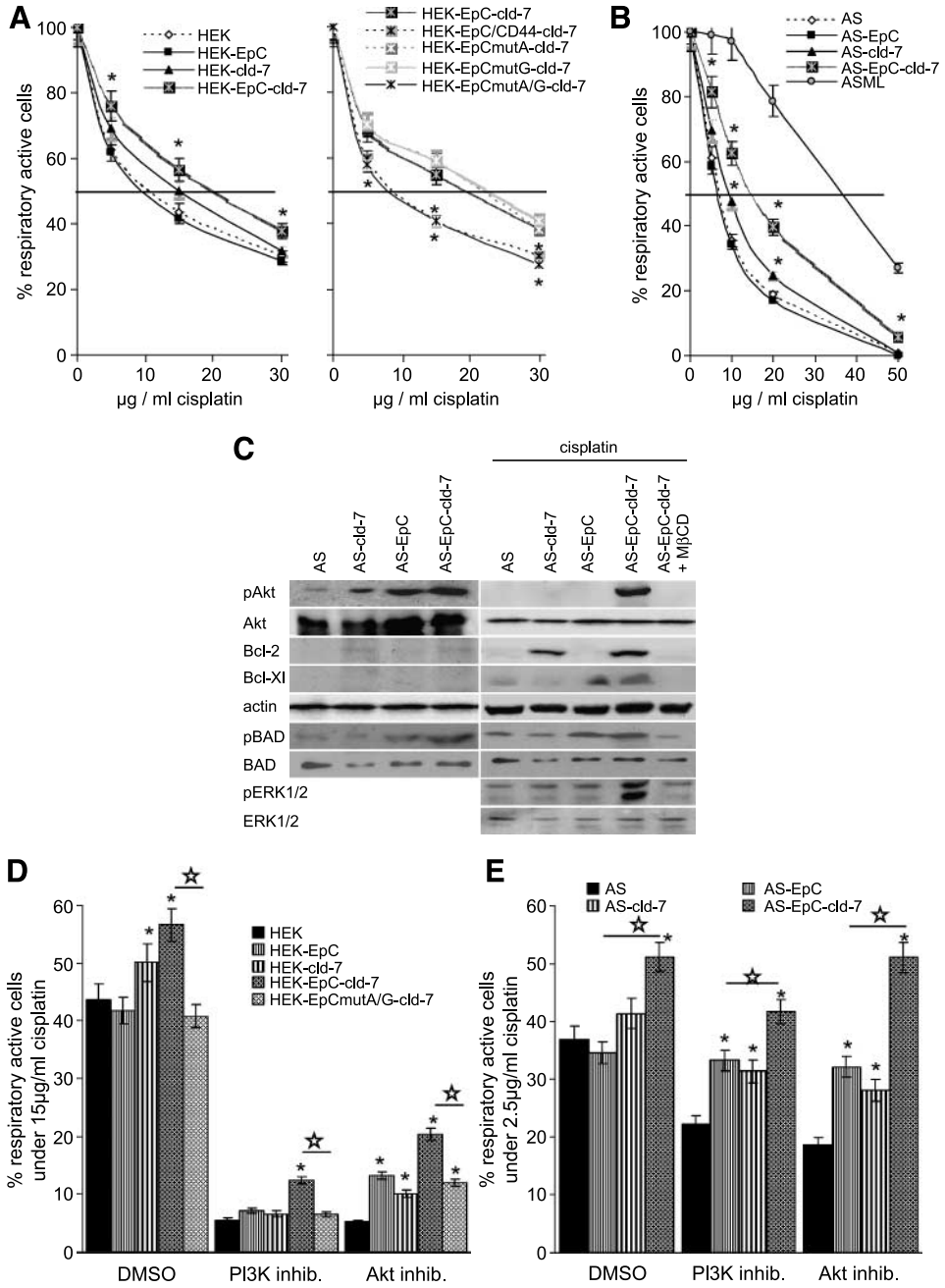

FIGURE 6. The effect of cld-7–associated EpC on tumor cell survival. **A.** HEK, HEK-EpC, HEK-cld-7, HEK-EpC-cld-7, and HEK-EpCmutA/G-cld-7 cells were cultured for 36 h in the presence of cisplatin. Points, mean relative percentage of respiratory active cells evaluated by MTT staining of triplicate experiments; bars, SD. **B.** AS, AS-EpC, AS-cld-7, and AS-EpC-cld-7 cells were cultured for 36 h in the presence of cisplatin. Points, mean relative percentage of respiratory active cells evaluated by MTT staining of triplicate experiments; bars, SD. **A** and **B.** The dose of cisplatin required for a 50% reduction in cell survival is indicated. *, significant differences between transfected and control HEK and AS cells. **C.** Cells described in **B** were lysed or were cultured for 48 h in the presence of 2.5 μg/mL cisplatin or (AS-EpC-cld-7 cells) were additionally treated with MβCD and lysed. Lysates were separated by SDS-PAGE. Transferred proteins were blotted with anti-Akt, anti-pAkt, anti–bcl-2, anti–bcl-xL, anti-BAD, anti-pBAD, and anti-actin (control). **D** and **E.** Cells described in **A** and **B** were cultured for 48 h in the presence of 10 μg/mL (HEK) or 2.5 μg/mL (AS) of cisplatin. Where indicated, the culture medium contained a phosphatidylinositol 3-kinase (*PI3K*) or Akt inhibitor. Relative respiratory activity (MTT staining) as compared with cells cultured in the absence of cisplatin. *, significant differences in the susceptibility of the transfected cells to the phosphatidylinositol 3-kinase and Akt inhibitor; ☆, significant differences between HEK-EpC-cld-7 and HEK-EpCmutA/G-cld-7 or AS-EpC and AS-EpC-cld-7.

whereas adhesion between AS-EpC cells is significantly augmented. D5.7 inhibits adhesion between AS-EpC cells but slightly strengthens adhesion between AS-EpC-cld-7 cells (Supplementary Fig. S2C and D).

Concomitantly with interfering with EpC-mediated cell-cell adhesion, the EpC-cld-7 complex promotes cell motility. This accounts for transwell migration and an *in vitro* wound healing assay. In both assays, migration of cells coexpressing EpC and cld-7 was increased, whereas EpC or cld-7 expression by itself or EpCmutA/G plus cld-7 had no significant effect on HEK (Fig. 4A and B) and AS cell migration (Supplementary Fig. S3A and B). The observation that D5.7 interferes with the migration of HEK-EpC-cld-7 cells supports the idea of an involvement of EpC. Notably, irrespective of cld-7 expression, EpC colocalizes with the actin cytoskeleton. However, cld-7 colocalizes with actin only when associated with EpC (Fig. 4C; Supplementary Fig. S3C).

Inhibition of EpC-mediated cell-cell adhesion and support of cell motility by EpC-associated cld-7 could promote the metastatic spread of tumor cells. In advance of controlling this hypothesis and because EpC has been described to support proliferation and apoptosis resistance (28-30), it became of interest to know whether these activities may also be linked to the association between EpC and cld-7.

Cld-7–Associated EpC Promotes Tumor Cell Proliferation and Survival

We already reported that the EpC-cld-7 complex is preferentially recovered in TEM (14). Evaluation of the TEM localization of EpC, EpCmutA, EpCmutG, and EpCmutA/G in HEK and HEK-cld-7 cells confirmed that EpC is recovered in the light fractions after sucrose gradient centrifugation only in the presence of cld-7. In HEK-EpCmutA/G-cld-7 lysates, where EpC does not associate with cld-7, EpC remains in the dense fraction. Similarly, AS-EpC-cld-7, but not AS-EpC or AS-cld-7, cells are TEM located (Fig. 5A). With TEM being known as a platform for signal transduction (36, 37), differences between AS-EpC and AS-EpC-cld-7 and particularly between HEK-EpC-cld-7 and HEK-EpCmutA/G-cld-7 cells could be indicative for strictly EpC-cld-7 complex–mediated functions related to the TEM recruitment.

EpC expression has no effect on the proliferative activity of AS cells and a slightly negative effect on HEK cell proliferation, whereas cld-7 expression promotes AS and HEK cell proliferation, which is accompanied by an increase in extracellular signal–regulated kinase (ERK)-1/2 phosphorylation. Particularly in AS cells, but also, albeit less pronounced, in HEK cells, proliferative activity is further increased by cld-7 together with EpC expression, which in both lines also strongly promotes ERK1/2 phosphorylation. The proliferative activity of HEK-EpCmutA-cld-7 or HEK-EpCmutG-cld-7 cells remains high, but the proliferative activity of HEK-EpCmutA/G-cld-7 cells does not exceed that of the parental HEK cells and ERK1/2 phosphorylation is strikingly reduced as compared with HEK-EpC-cld-7 cells (Fig. 5B and C). Anti-EpC (D5.7), added to the culture medium, exerted no major effect on the proliferation of HEK-EpC, HEK-EpC-cld-7, or HEK-EpCmutA/G-cld-7 cells (data not shown). To control for the suggested linkage between proliferative activity and ERK1/2 phosphorylation, proliferative activity was evaluated in the presence of a medium dose of a mitogen-activated protein kinase/ERK kinase (MEK)-1/2 inhibitor (SL327), which sufficed to reduce the proliferative activity of untransfected, EpC-transfected, and EpCmutA/G-cld-7–transfected HEK and AS cells by roughly 40%. The inhibitory effect on HEK-cld-7 and AS-cld-7 cells was weaker (20-30% inhibition). However, this medium dose of SL327 had no effect on the proliferative activity of HEK-EpC-cld-7 and AS-EpC-cld-7 cells (Fig. 5D). We interpret the findings in the sense that EpC-cld-7–promoted proliferation may, at least in part, rely on the EpC-cld-7 association and the TEM localization of the complex.

Differences in drug resistance were evaluated by proliferative activity, cell death (data not shown), and respiratory activity and in the presence of increasing doses of cisplatin. All three assays revealed comparable results. HEK-EpC-cld-7 cells display higher and HEK-cld-7 cells slightly higher cisplatin resistance than HEK or HEK-EpC cells. Increased apoptosis resistance is lost in HEK cells transfected with EpCmutA/G-cld-7 or EpC/CD44chim-cld-7 (Fig. 6A). AS-EpC-cld-7 cells also showed higher apoptosis resistance than mock transfected AS or AS-EpC cells. In AS cells, too, cld-7 expression by itself leads to a slight increase in drug resistance (Fig. 6B).

Evaluation of Akt phosphorylation as well as of antiapoptotic protein expression in AS, AS-EpC, AS-cld-7, and AS-EpC-cld-7 revealed slightly increased phosphorylation of Akt and significantly increased BAD phosphorylation in AS-EpC, and more pronounced in AS-EpC-cld-7 cells (Fig. 5C). Importantly, cisplatin treatment led to further increase of Akt phosphorylation and induction of bcl-2 and bcl-xL in AS-EpC-cld-7 cells. Bcl-2 expression was also seen in AS-cld-7 cells, and low-level bcl-xL expression in AS-EpC cells. Akt activation as well as bcl-2 and bcl-xL expression and BAD phosphorylation in cisplatin-treated AS-EpC-cld-7 cells essentially depended on TEM localization. All these changes were largely abolished by MβCD treatment. The latter also accounted for ERK1/2 phosphorylation, which was very strong in cisplatin-treated AS-EpC-cld-7 cells but hardly detectable after MβCD treatment (Fig. 6C).

These findings correlate well with a higher percentage of respiratory active HEK-EpC-cld-7 and AS-EpC-cld-7 than of HEK and AS cells when cultured in the presence of cisplatin and either a phosphatidylinositol 3-kinase or an Akt inhibitor. It should be noted that AS cells are less sensitive to phosphatidylinositol 3-kinase and Akt inhibition than HEK cells and that AS-EpC cells, also different from HEK-EpC cells, are less susceptible to the phosphatidylinositol 3-kinase inhibitor than nontransfected cells. Nonetheless, AS-EpC cells are still significantly more susceptible than AS-EpC-cld-7 cells (Fig. 6D and E).

Taken together, cld-7–associated EpC induces proliferation, likely via the mitogen-activated protein kinase pathway, and supports activation of the mitochondrial pathway of apoptosis resistance.

The EpC-Cld-7 Association Supports Tumorigenicity and Tumor Cell Dissemination

HEK cells were transfected with (mutated) *EpC* and/or *cld-7* cDNA, which allowed to evaluate a possible effect of the

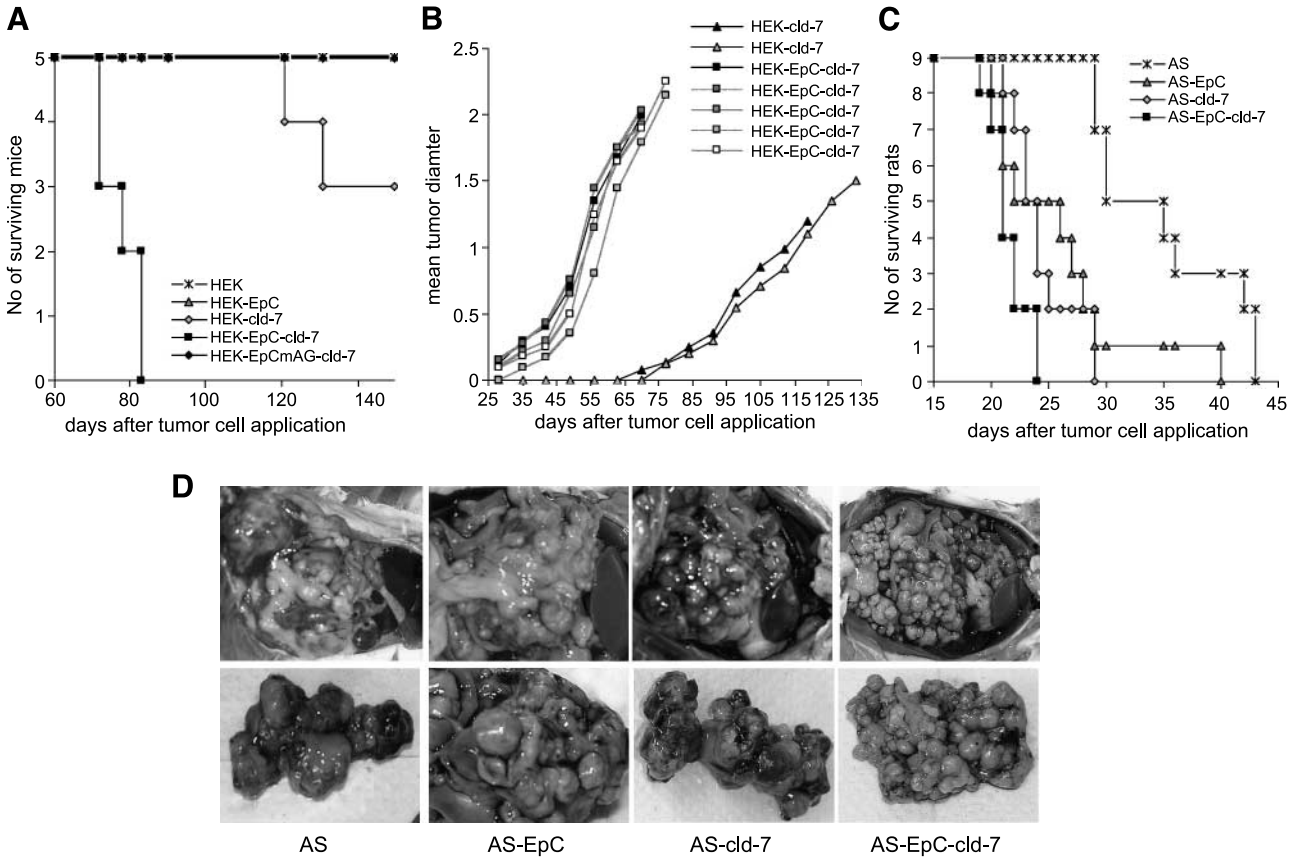

Figure 7. Impact of the EpC-cld-7 association on *in vivo* tumor growth. **A** and **B.** Nude mice received an intraperitoneal injection of HEK, HEK-EpC, HEK-cld-7, HEK-EpC-cld-7, or HEK-EpCmutA/G-cld-7 cells (5×10^6). Number of surviving mice (**A**) and tumor growth (**B**) during an observation period of 20 wk. **C** and **D.** BDX rats received an intraperitoneal injection of AS, AS-EpC, AS-cld-7, or AS-EpC-cld-7 cells (5×10^5). Survival time (**C**) and macroscopic appearance (**D**) of the tumors.

EpC-cld-7 expression on tumorigenicity. HEK, HEK-EpC, HEK-EpC-cld-7, and HEK-EpCmutA/G-cld-7 cells were injected intraperitoneally into nude mice. Mice receiving HEK-EpC-cld-7 cells were sacrificed 8 to 9 weeks after tumor cell application, when the tumors reached a mean diameter of 2 cm. Two mice receiving HEK-cld-7 cells started to develop tumors after 9 weeks and were sacrificed after 16 to 19 weeks. All remaining mice were sacrificed after 20 weeks and were tumor-free (Fig. 7A and B). The HEK-EpC-cld-7 and HEK-cld-7 tumor–bearing mice developed a single, solid intraperitoneal

Table 1. Tumor Growth–Promoting Features of the EpC-Cld-7 Complex

(A) EpC-cld-7 Promotes Solid and Ascitic Tumor Growth

Tumor Line*	Survival Time (d) †	*P*	Ascites (mL)	*P*
AS-mock	35.2 ± 6.1		2.3 ± 1.2	
AS-EpC	26.0 ± 6.2	0.0061	5.3 ± 1.4	0.0025
AS-cld-7	24.4 ± 2.8	0.0002	4.3 ± 0.7	0.0105
AS-EpC-cld-7	21.6 ± 1.7	<0.0001	6.3 ± 1.0	0.0003

(B) D5.7 Interferes with the Intraperitoneal Growth of AS-EpC and AS-EpC-cld-7 Cells

Tumor Line*	Treatment ‡	Survival Time (d) †	*P*	Ascites (mL)	*P*	Distant Metastasis
AS-EpC	mIgG	26.1 ± 6.0		5.5 ± 1.5		
AS-EpC	D5.7	39.4 ± 8.8	0.0060	3.9 ± 0.8	0.0424	thymus (1/9)
AS-EpC-cld-7	mIgG	21.2 ± 1.9		6.5 ± 1.1		
AS-EpC-cld-7	D5.7	27.2 ± 6.4	0.0199	4.6 ± 0.8	0.0165	thymus (7/9)

*Rats received 5×10^5 tumor cells intraperitoneally.
† Survival time corresponds to the time when rats had to be sacrificed according to the tumor load.
‡ Rats received 100 μg mIgG or D5.7, intraperitoneally, twice a week.

nodule that infiltrated the muscles of the peritoneal wall and showed a central necrotic area. Neither macroscopic inspection nor *in vitro* culture of dispersed tissues revealed evidence for distant metastasis formation in lymph nodes, liver, or lung (data not shown). Taken together, the *in vivo* growth of HEK-EpC-cld-7 cells, but not of HEK-EpC cells, indicates that the EpC-cld-7 complex supports tumorigenicity.

Several clinical studies report on convincing therapeutic efficacy of EpC-specific antibodies, particularly with respect to a reduction in ascitic load (35, 39-44). Hence, we finally asked whether coexpression of cld-7 alters the growth profile of EpC-expressing tumor cells and whether the therapeutic efficacy of EpC-specific antibodies correlates with the EpC-cld-7 association. BDX rats received an intraperitoneal injection of 5×10^5 AS, AS-EpC, AS-cld-7, and AS-EpC-cld-7 cells. Starting 2 days after tumor cell injection, rats received intraperitoneal injections of 100 μg mouse IgG (control) or D5.7 twice per week. AS-EpC−, AS-cld-7−, and AS-EpC-cld-7−bearing rats developed large tumors and were sacrificed after a significantly shorter period than AS-bearing rats, with AS-EpC-cld-7−bearing rats having the shortest "survival time" (Fig. 7C; Table 1A). AS, AS-EpC, and AS-cld-7 cells grew as solid tumor nodules. AS-EpC-cld-7 cells grew as solid tumors composed of multiple small nodules (Fig. 7D). AS-cld-7 tumors were very poorly vascularized and AS-EpC-cld-7 tumors showed good vascularization only in the subcapsular region (Fig. 8A). In addition, as shown for $CD8^+$ and $CD11b^+$ cells, AS and AS-EpCAM tumors were infiltrated by T cells and monocytes, whereas AS-EpCAM-cld-7 tumors hardly contained any T cells but most abundantly contained monocytes. Anti-EpCAM treatment of AS-EpC− or AS-EpC-cld-7−bearing rats was accompanied by a further increase in monocytes (Fig. 8B), but not T cells (data not shown), in the tumor tissue. AS-bearing rats developed comparably little ascitic fluid, whereas AS-EpC−, AS-cld-7−, and particularly AS-EpC-cld-7−bearing rats developed large amounts of bloody ascites (Table 1A) with a high load of dispersed tumor cells (data not shown). Anti-EpC (D5.7) application did not hamper the solid tumor growth of AS and AS-cld-7 cells (data not shown), whereas the ascitic load of AS-EpC− and AS-EpC-cld-7−bearing rats was significantly reduced and the survival time became significantly prolonged. However, D5.7-treated AS-EpC-cld-7−bearing rats developed metastasis in the thymus (seven of nine rats). Thymic metastases were not seen in control IgG−treated rats and only in one of nine D5.7-treated AS-EpC−bearing rats (Table 1B). Thymic epithelial cells also express EpC and are supposed to support thymocyte maturation. Thus, it was interesting to see that the few remaining thymocytes in the metastatic organ formed small clusters between the tumor cells (Fig. 8C).

Taken together, the association of EpC with cld-7 significantly increases the tumorigenicity and aggressiveness of tumor

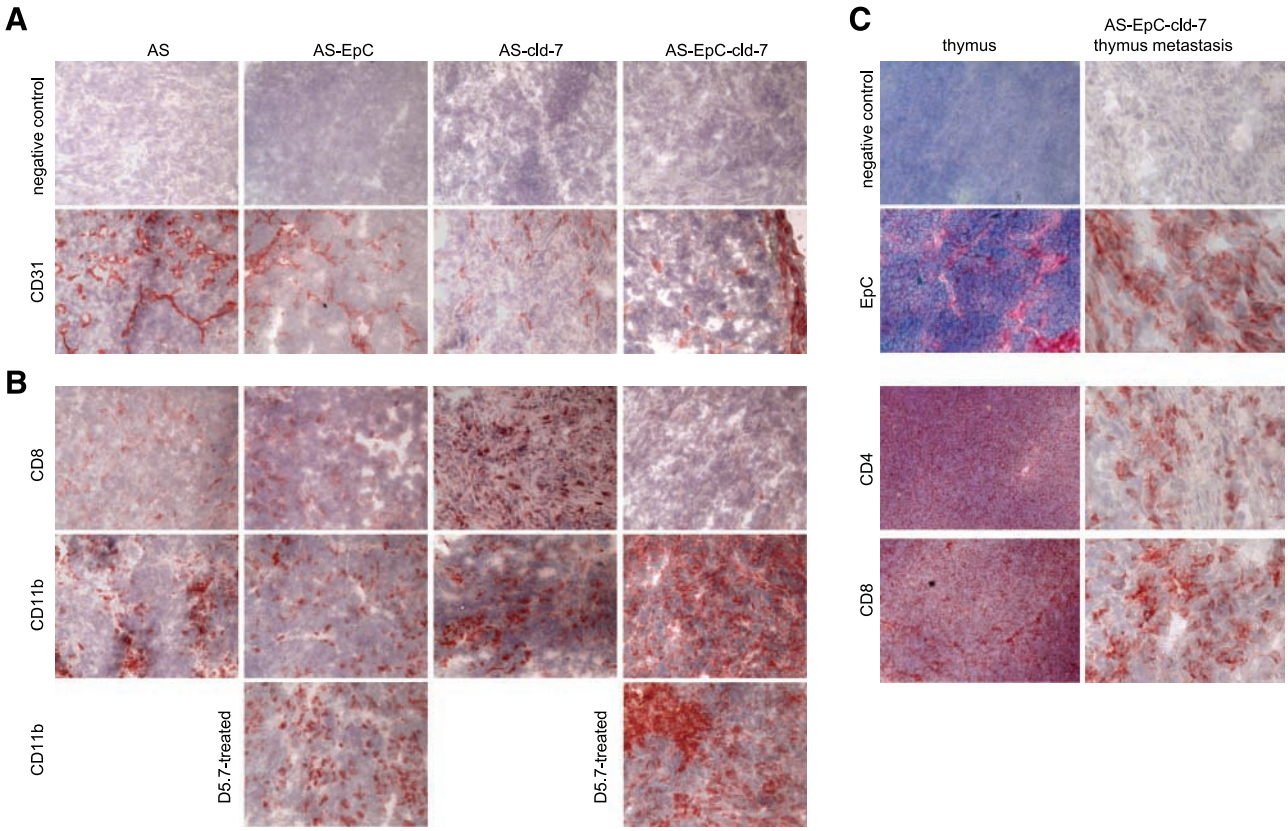

Figure 8. Vascularization, leukocyte infiltration, and metastasis formation of AS-EpC-cld-7 tumors. **A** and **B.** AS, AS-EpC, AS-cld-7, or AS-EpC-cld-7 tumors were shock-frozen and 5-μm slices were stained with anti-CD31 (**A**) and anti-CD8 and anti-CD11b (**B**). **C.** Staining of 5-μm slices of a shock-frozen normal rat thymus and a thymic metastasis of AS-EpC-cld-7 with D5.7, CD4, and anti-CD8. Bar, 0.4 μm.

growth. Distinct to our expectation, the therapeutic efficacy of D5.7 does not seem to be influenced, at least in the AS model, by the concomitant presence of cld-7. However, D5.7 promotes rather selectively the growth of AS-EpC-cld-7 cells in the thymus.

Discussion

EpC frequently is overexpressed in carcinoma (1-12). It has been suggested to support tumor growth by interfering with E-cadherin–mediated adhesion (3, 39) and by promoting up-regulation of c-myc expression (30). The underlying mechanisms have not been fully uncovered. We noted that EpC can associate with cld-7 (14, 34). Notably, EpC and cld-7 also display striking colocalization in hepatic progenitor cells with repopulating capacity (40). Colocalization in tumor cells and progenitor cells suggests that this association may have a major effect on EpC-mediated functions. Indeed, the EpC-cld-7 complex promotes cell motility, proliferation, survival, tumorigenicity, and metastasis formation.

The Transmembrane Domain of EpC Associates with Cld-7

EpC coimmunoprecipitates with cld-7 after treatment with a membrane-permeable, but not a membrane-impermeable, cross-linker (34). This finding suggested that EpC and cld-7 do not associate via their extracellular domains. In fact, EpCΔEGF/TG coimmunoprecipitates with cld-7. However, the conformation of the extracellular domains of EpC contributes to the association. Although N-glycosylation of EpC is not required, a conformational change by 2-mercaptoethanol treatment prevents the EpC-cld-7 association. The two molecules also associate after deletion of the cytoplasmic tail of EpC or the COOH-terminal cytoplasmic tail of cld-7. However, a chimeric molecule composed of the extracellular domains of EpC and the transmembrane and cytoplasmic domains of CD44 does not coimmunoprecipitate with cld-7. The transmembrane domains of both molecules do not contain charged amino acid residues that could account for transmembrane associations. However, both the transmembrane domain of EpC and the 4th transmembrane domain of cld-7 contain the AxxxA/G motif that can support protein-protein associations (38, 41). Although an exchange of the small amino acid A279 or G282 within this motif in EpC does not prevent the association with cld-7, cld-7 does not associate with EpC after exchange of both A279 and G282 to I279 and I282. Thus, the AxxxG motif in the transmembrane domain of EpC is required for the association with cld-7.

Considering possible functional consequences of the EpC-cld-7 association, it is important to note that the EpC-cld-7 complex is located in glycolipid and TEM, which harbor linker and signal transduction molecules, allowing these membrane domains to function as a signaling platform (35-37, 42). Notably, both molecules EpC and cld-7 by themselves reside in the more fluid phase of the cell membrane (14), even when coexpressed, but their association is being prevented by the A and T mutation in the EpC molecule. We do not yet know whether EpC-cld-7 associates with cell-cell adhesion sites. This will be important to evaluate because tight junction proteins have repeatedly been reported to be engaged in the nucleo-junctional interplay, which includes induction of gene transcription (43), a process that might be initiated via the EpC-cld-7 association in TEM. HEK-EpCmutA/G-cld-7 cells will provide an optimal tool to search for functions essentially depending on the EpC-cld-7 complex.

Cld-7–Associated EpC Promotes Migration, Proliferation, and Drug Resistance

Expression of the EpC-cld-7 complex in pancreatic and colorectal tumors (14, 34) suggested the association to be advantageous for tumor growth or progression. In fact, cld-7 interferes with EpC oligomerization, which is a prerequisite for EpC-mediated homophilic cell adhesion (22). As a consequence, the tight membrane interactions between HEK-EpC and AS-EpC cells are not seen in HEK-EpC-cld-7 and AS-EpC-cld-7 cells. HEK-EpC-cld-7 or AS-EpC-cld-7 cells also do not agglomerate; homophilic cell-cell adhesion is strongly reduced; and the cells adhere more readily to plastic. Reduced cell-cell adhesion is accompanied by increased cell motility, which becomes efficiently inhibited by an EpC-specific antibody. Because colocalization of cld-7 with actin bundles is only seen in cells expressing the EpC-cld-7 complex, it is tempting to speculate that increased motility is supported by this cld-7-actin association via EpC.

Formation of the EpC-cld-7 complex has bearing on cell cycle progression and drug resistance. HEK-EpC-cld-7 cells display increased cisplatin resistance as compared with HEK-EpCmutA/G-cld-7 cells. Thus, neither EpC nor cld-7, but only the TEM-located EpC-cld-7 complex accounts for apoptosis resistance. AS-EpC-cld-7 cells also are more apoptosis resistant than AS-EpC or AS-cld-7 cells. Apoptosis resistance is accompanied by a strong up-regulation of Akt phosphorylation and an increase in the antiapoptotic proteins bcl-2 and bcl-xL and pronounced inactivation of the proapoptotic protein BAD by phosphorylation, which confirm the EpC-cld-7 association to be decisive for the strength of drug resistance. Furthermore, expression of the EpC-cld-7 complex is accompanied by accelerated cell cycle progression and a constitutive increase in ERK1/2 phosphorylation. As revealed by MβCD treatment, both EpC-cld-7 complex–induced ERK1/2 phosphorylation and the activation of antiapoptotic signaling essentially depend on the TEM localization of the complex. Experiments to unravel the signal transduction cascades that are initiated by the GEM-localized EpC-cld-7 complex are in progress.

Our findings show that the EpC-cld-7 association is involved in drug resistance and accelerated cell cycle progression, activities that have been associated with EpC overexpression (35) and are tumor growth promoting. In addition, cld-7 interferes with EpC-mediated cell-cell adhesion, which could explain that up-regulated expression of the cell-cell adhesion molecule EpC on tumor cells does not prohibit tumor cell dissemination as long as the cells coexpress cld-7.

The Tumor Growth–Promoting Features of EpC Rely on the Association with Cld-7

Strongest evidence that the EpC-cld-7 complex promotes tumorigenicity derives from the growth of HEK-EpC-cld-7 cells in five of five nude mice. HEK-cld-7 cells formed tumors in two of five mice, whereas mock-transfected HEK cells and

HEK cells expressing EpC or EpCmutA/G-cld-7 did not grow. AS-EpC, AS-cld-7, and, most pronounced, AS-EpC-cld-7 cells showed accelerated *in vivo* growth as compared with mock-transfected cells. In addition, AS-EpC-cld-7 cells stimulated ascitic growth more efficiently than AS, AS-EpC, and AS-cld-7 cells. Pronounced ascitic growth of AS-EpC-cld-7 cells is well in line with the reduced capacity for homophilic cell-cell adhesion. It also argues for improved survival of the isolated tumor cell. Furthermore, AS and AS-EpC cells form one big tumor mass with a rim of live tumor cells surrounding a central necrotic area. AS-cld-7 cells form smaller nodules that were, however, poorly vascularized and also showed central necrosis. AS-EpC-cld-7 cells grew in multiple small nodules that were well vascularized only in the subcapsular region. Likely due to the small size of the individual nodules, AS-EpC-cld-7 tumors did not contain necrotic areas. The multiple small nodules also argue for a higher *in vivo* cloning efficacy than the outgrowth of one big tumor mass of AS and AS-EpC cells. Thus, the EpC-cld-7 complex supports tumorigenicity and tumor cell survival, where accelerated cell cycle progression may well contribute.

Anti-EpC has been reported to be of therapeutic efficacy in several types of human cancer (35, 44-49). The most striking effect was observed with a bispecific antibody on ascites production by ovarian cancer (46). The underlying mechanism remains largely elusive. We speculated that cld-7–associated monomeric EpC may be more accessible for EpCAM-specific antibodies. This apparently is not the case for the D5.7 anti-EpC antibody. Although the EpC-specific antibody D5.7 interferes more efficiently with the ascitic growth than with the growth of the solid tumor mass, D5.7 affects ascites production by AS-EpC-cld-7 and AS-EpC cells to a comparable degree. We do not know the D5.7 epitope. However, because D5.7 does not recognize oligomeric EpCAM, it may recognize the TG domain, required for lateral association, but not the EGF-like domain required for the reciprocal interaction (22). A higher efficacy of D5.7 binding to the EpCAM-cld-7 complex could explain the stronger agglomeration of EpCAM-cld-7–transfected cells in culture due to antibody cross-linking of neighboring cells. On the other hand, adhesion of HEK-EpC and AS-EpC cells to an adherent monolayer was inhibited when cells were preincubated with D5.7, which may be explained by no free antibody binding site being available for antibody cross-linking. Yet, this finding may not be relevant for the *in vivo* situation. Instead, although *in vivo* the D5.7 concentration may be too low for cross-linking tumor cells, it may suffice to arm macrophages and natural killer cells that serve to attack AS-EpCAM as well as AS-EpCAM-cld-7 cells (50). Further experiments are required to support the hypothesis. At present, we can only state that D5.7 interferes with ascitic growth of AS-EpC and AS-EpC-cld-7, whereby cld-7 interfering with EpC oligomerization may not significantly contribute to the therapeutic efficacy of D5.7.

Instead, D5.7 promotes metastasis formation in the thymus of AS-EpC and, far more pronounced, AS-EpC-cld-7 cells. Thus far, we have no explanation. It is interesting to note that thymic epithelial cells, which form a well-organized network, also express EpC (51-54). Although EpC knockout mice did not reveal severe defects in thymocyte maturation, it has been shown that EpC is essential for the organization of the architecture of the thymic epithelium, which should support thymocyte maturation (54, 55). We noted that D5.7 strengthens the adhesion of AS-EpC-cld-7 cells to AS-EpC cells. Thus, we hypothesize that D5.7 acts as a linker between the tumor and surrounding cells. Depending on the targeted cells, the tumor cell may become lysed or receive survival and growth-promoting signals. Whereas in the peritoneal cavity, macrophages are recruited that obviously contribute to tumor cell damage, the EpC-cld-7–expressing tumor cells may have a growth advantage after settlement in the thymus, as was suggested for early thymocyte progenitors, which also express EpC (51-53). As markers of hepatic progenitor cells with repopulating capacity (40), the EpC-cld-7 complex might also promote stem cell/cancer-initiating cell communication with niche elements. This hypothesis remains to be consolidated. We also do not yet know why and by which mechanisms D5.7 drives AS-EpC and, more efficiently, AS-EpC-cld-7 cells into the hardly accessible thymic organ (56).

In conclusion, an EpC-cld-7 complex, rather than EpC by itself, supports migration, drug resistance, proliferation, and tumorigenicity. Furthermore, an EpC-specific antibody apparently facilitates the cross talk between EpC/EpC-cld-7–expressing tumor cells and surrounding tissue such that the tumor cell receives death or, for example, within the thymic environment, growth-promoting signals. A cross talk between EpC-cld-7-complex–expressing cells and the surrounding tissue may also be of relevance for cancer-initiating cells.

Materials and Methods

Cell Lines

The rat pancreatic adenocarcinoma cell lines BSp73AS (AS) and BSp73ASML (ASML; ref. 57) were grown in RPMI medium supplemented with antibiotics, L-glutamine, and 10% FCS (RPMI-s). HEK293 (HEK) cells (58) were grown in DMEM supplemented with antibiotics, L-glutamine, and 15% FCS (DMEM-s). AS and HEK cells were stably or transiently transfected with the rat cDNA of *EpC* (32), *cld-7* (34), or both using the pcDNA3.1(+) vector that carries either the neomycin or hygromycin resistance cDNA. HEK cells were also transfected with the following mutated cDNA: *EpCΔEGF/TG-myc*; *EpCΔcyt*; *EpC-CD44chim*, where the transmembrane and cytoplasmic domains of EpC have been replaced by the transmembrane and cytoplasmic domains of CD44; *EpC-mutA279* (*EpCmutA*); *EpCmutG282* (*EpCmutG*); *EpC-mutA279/G282* (*EpCmutA/G*); and *cld-7Δcyt-myc*. The following primers have been used: EpC forw, 5′-TATAAAG-CTTGCCACCATGGCGCCCCCCAAGGCCCTC-3′; EpC rev, 5′-TTGCTCCATGTCTTTCTGAGCTGCGGCCAG-3′; Ep-CΔEGF/TG-myc forw, 5′-GACCGGCGTCGAGTCTTTCTG-AGGCTCTCT-3′; EpCΔEGF/TG-myc forw, 5′-AGAAAGAC-TCCGAGAGAGTGAGGACCTACT-3′; EpCΔcyt rev, 5′-TATATACTCGAGTCATGTAGATATAACCAGGACA-AC-3′; EpC-A279I, 5′-CGCCGTCATTGTCGTGGTGGTGT-TAATAGTCATTGCG-3′; EpC-G283I, 5′-AGTCATTGCGGG-GATTGTTGTCCTGGTTATAT-3′; cld-7 forw, 5′-ATATAAAGC TTACCACCATGGCTAACTCGGGCCTGCAA-3′; cld-7 rev, 5′-TATATAGGATCCTCAC ACGTATTCCTTAGAGGA-3′; Myc-cld-7 forw, 5′-TATATAGGATCCATGGCTAACTCG

GGCCTGCAA-3′; Myc-cld-7 rev, 5′-TATATAAAGCTTTCA-CACGTATTCCTTAGAGGA-3′; Myc-cld-7Δcyt rev, 5′-TATA-TAAAGCTTTCAGGGGCAGGAGCAAGAGAGCAG-3′; CD44-TM/cyt forw, 5′-TCCATGCAGATTCCAGAGTGGCT-TATCATC-3′. All cDNA inserts were controlled by sequencing. Expression was controlled by flow cytometry. Mock-, EpC-, and cld-7–transfected AS and HEK cells were maintained in RPMI-s or DMEM-s with 500 μg/mL G418 or 150 μg/mL hygromycin. Confluent cultures were trypsinized, split, and replated.

Antibodies

The following antibodies were used: mouse anti-rat EpC (D5.7; ref. 57), anti–transferrin receptor (American Type Cell Culture Collection), and guinea pig anti-human cld-7, raised against the COOH-terminal domain (60). Hybridoma culture supernatants were purified by passage over protein G-Sepharose and, where indicated, were labeled with biotin or FITC. Anti-mouse and anti-rat CD8, CD11b, CD31, Gr-1, ERK1/2, pERK1/2, Akt, pAkt, bcl-2, bcl-xL, BAD, pBAD, actin, and dye-labeled secondary antibodies and streptavidin were obtained commercially (BD/Pharmingen and Dianova).

Flow Cytometry

Tumor cells (1×10^5) were stained according to routine protocols. Before staining, trypsinized cells were allowed to recover for 2 h at 37°C in RPMI-s. For intracellular staining (cld-7), cells were fixed and permeabilized. Apoptosis was evaluated by staining with Annexin V-FITC and propidium iodine. Samples were analyzed using a FACSCalibur (BD).

Histology and Immunofluorescence Microscopy

Cryostat sections (5 μm) of snap frozen tissue were fixed in chloroform/acetone (1:1) for 4 min and stained with the primary antibody or were fixed (4% paraformaldehyde), permeabilized (0.1% Triton X-100, 4 min, 4°C), and stained with anti–cld-7 (1 h), biotinylated secondary antibodies (30 min), and alkaline phosphatase–conjugated avidin-biotin complex solution (5-20 min). Sections were counterstained with Mayer's hematoxylin. For negative controls, the primary antibody was replaced with normal mouse or guinea pig immunoglobulin.

In colocalization studies, cells grown on glass slides were fixed and permeabilized as described above. Cells were incubated with phalloidin-FITC and anti-EpC or anti–cld-7 (60 min, 4°C) and Cy3-labeled anti-mIgG or biotinylated anti–guinea pig IgG (60 min, 4°C) and Cy3-labeled streptavidin (60 min, 4°C). Slides were mounted in Elvanol. Digitized images were generated using a Leica DMRBE microscope (Carl Zeiss). In double-staining experiments, images were digitally overlaid.

Chemical Cross-linking

For cross-linking, cells or lysates were treated with the membrane-permeable chemical cross-linker dithio-bis-succinimidylproprionate (1 mmol/L in HEPES buffer, 30 min, room temperature), followed by quenching with 200 mmol/L glycine in PBS (pH 7.2) for 15 min.

Immunoprecipitation

Cells (10^7) were scraped in lysis buffer [25 mmol/L HEPES (pH 7.2), 150 mmol/L NaCl, 5 mmol/L $MgCl_2$, 2 mmol/L phenylmethylsulfonylfluoride, protease inhibitor mix and 1% Lubrol]. After incubation for 1 h at 4°C, lysates were centrifuged at 20,000 × *g* for 10 min at 4°C. For immunoprecipitation, precleared (1/10 volume protein G-Sepharose, 1 h, 4°C; Amersham Pharmacia) lysates were incubated for 1 h at 4°C with the indicated antibodies, followed by 4-h incubation with protein G-Sepharose. Immune complexes were washed four times with ice-cold lysis buffer. Immunoprecipitated proteins were analyzed by SDS-PAGE followed by Western blotting.

Western Blotting

Lysates and immunoprecipitates were resuspended in nonreducing sample buffer and heated 5 min at 95°C before loading on a polyacrylamid gel. Where indicated, cells were treated with tunicamycin (5 μg/mL, overnight, 37°C) or 2-mercaptoethanol (50 mmol/L, 30 min, 37°C). Proteins were separated by SDS-PAGE and subsequently transferred onto a nitrocellulose membrane (Amersham Pharmacia) by electroblotting. Membranes were blocked with 5% low fat milk (Roth) and 0.1% Tween 20 (Sigma) and were probed with the antibodies. Blots were visualized by chemiluminescence (ECL kit, Amersham Pharmacia).

Sucrose Density Gradient

Cells were lysed in 1% Lubrol. After centrifugation (10 min, 20,000 × *g*), lysates were adjusted to 40% sucrose in HEPES buffer in a total volume of 4.5 mL. Lysates were layered on 1.3 mL 50% sucrose and were overlaid with 2.3 mL 30%, 2.3 mL 20%, and 1.3 mL 5% sucrose. After centrifugation (200,000 × *g*, 16 h), 12 fractions were collected from the top of the tubes. Fractions were resuspended in lysis buffer.

Apoptosis and Proliferation

Tumor cells (5×10^4) were seeded in flat-bottomed 96-well plates. After settling, serial dilutions of cisplatin (starting concentration: 35 μg/mL) in RPMI-s were added. Cells were cultured for 24 to 72 h. The percentage of respiratory active cells was evaluated by MTT (3-4,5-dimethylthiazol-2-yl-2,5-diphenyl-tetrazolium bromide) staining. The color reaction (550 nm) was measured in an ELISA reader. Proliferation was evaluated by [^{3}H]thymidine incorporation. Cells (5×10^3) were seeded in triplicates in flat-bottomed 96-well plates. Cells were cultured for 24 h and [^{3}H]thymidine (10 μCi/mL) was added during the last 8 h of culture. Plates were harvested with an automatic harvester and [^{3}H]thymidine incorporation was determined in a beta-counter. Where indicated, proliferation and/or apoptosis was evaluated in the presence of the MEK1/2 inhibitor SL327 (5 μmol/L), the phosphatidylinositol 3-kinase inhibitor LY294002 (5 μmol/L), or Akt inhibitor II (10 μmol/L).

Agglomeration

Tumor cells (1×10^6) were resuspended in 1 mL RPMI-s, seeded in 24-well plates, and incubated on a rocking platform. Agglomeration was microscopically evaluated after 1 h. After an additional 12-h incubation without rocking, the stability of agglomeration was reevaluated.

Adhesion

In cell-cell adhesion assays, cells were labeled with carboxyfluorescein diacetate succinimidyl ester and were seeded (1×10^5 per well) in triplicates on a monolayer of cells in 96-well plates. Where indicated, cells were preloaded with antibody (10 μg/mL, 30 min, 4°C). After incubation (2 h, 37°C), nonadherent cells were removed by washing. Absorbance of adherent, carboxyfluorescein diacetate succinimidyl ester–labeled cells was measured at 535 nm.

Cell Migration

Cells (5×10^4) were loaded with antibody (10 μg/mL, 30 min, 4°C) and seeded in the upper part of a Boyden chamber in 30 μL RPMI/0.1% bovine serum albumin in triplicates. The lower chamber, separated by a 8-μm-pore-size polycarbonate membrane, contained 30 μL RPMI/10% FCS. Migration was evaluated after 24 h. After removing nonmigrated cells from the upper side of the membrane, migrated cells at the lower side of the membrane were fixed and stained (10% formaldehyde, 0.1% crystal violet). After washing and lysis in 10% acetic acid, absorbance was measured in an ELISA reader at 595 nm. Migration is presented as percentage of migrating cells, taking the starting load as 100%. Alternatively, cells were seeded in 1-cm Petri dishes. At subconfluence, the monolayer was scratched with a pipette tip. Medium was exchanged and wound healing was followed for 48 h. Healing was documented using an inverted microscope.

In vivo *Metastasis Assay*

HEK-mock, HEK-EpC, HEK-cld-7, HEK-EpC-cld-7, and HEK-EpCmutA/G-cld-7 cells (5×10^6) were suspended in 200 μL PBS and injected intraperitoneally into nu/nu mice. AS-mock, AS-EpC, AS-cld-7, and AS-EpC-cld-7 cells (5×10^5) were injected intraperitoneally into syngeneic BDX rats. Rats received concomitantly with the tumor and thereafter 100 μg control IgG or D5.7 twice a week. Mice and rats were controlled weekly for the development of ascites and/or a solid tumor mass in the peritoneal cavity. Animals were sacrificed 20 wk after tumor cell application or when the intraperitoneal tumor reached a palpable size or when developing ascites.

At autopsy (nu/nu and rats), the mean diameter of solid tumors in the peritoneal cavity and/or the volume of ascites was determined. Animals were macroscopically evaluated for the presence of metastases. Lymph nodes, liver, and lung were also dispersed and cell suspensions were cultured for 3 wk to observe potential tumor cell outgrowth. Shock-frozen sections of the solid tumors were subjected to immunohistologic staining. Animal experiments were approved by the local governmental authorities.

Statistics

Functional *in vitro* assays were repeated at least thrice. Mean values are based on triplicates. Significance of differences was calculated by the Student *t* test. Statistical significance of *in vivo* assays was evaluated by the Wilcoxon rank sum test for two-group comparisons of quantitative variables. All tests were done two-sided to the 0.05 level.

Disclosure of Potential Conflicts of Interest

No potential conflicts of interest were disclosed.

References

1. Momburg F, Moldenhauer G, Hämmerling GJ, et al. Immunohistochemical study of the expression of a M_r 34,000 human epithelium-specific surface glycoprotein in normal and malignant tissues. Cancer Res 1987;47:2883–91.

2. Bergsagel PL, Victor-Kobrin C, Brents LA, et al. Genes expressed selectively in plasmacytomas: markers of differentiation and transformation. Curr Top Microbiol Immunol 1992;182:223–8.

3. Balzar M, Winter MJ, de Boer CJ,Litvinov SV. The biology of the 17-1A antigen (Ep-CAM). J Mol Med 1999;77:699–712.

4. Gastl G, Spizzo G, Obrist P. Dunser M, Mikuz G. Ep-CAM overexpression in breast cancer as a predictor of survival. Lancet 2000;356:1981–2.

5. Braun S, Pantel K. Prognostic significance of micrometastatic bone marrow involvement. Breast Cancer Res Treat 1998;52:201–16.

6. Litvinov SV, van Driel W, van Rhijn CM, et al. Expression of Ep-CAM in cervical squamous epithelia correlates with an increased proliferation and the disappearance of markers for terminal differentiation. Am J Pathol 1996;148: 865–75.

7. Ruck PP, Wichert G, Handgretinger R, Kaiserling E. Ep-CAM in malignant liver tumours. J Pathol 2000;191:102–3.

8. Seligson DB, Pantuck AJ, Liu X, et al. Epithelial cell adhesion molecule (KSA) expression: pathobiology and its role as an independent predictor of survival in renal cell carcinoma. Clin Cancer Res 2004;10:2659–69.

9. Went PT, Lugli A, Meier S, et al. Frequent EpCam protein expression in human carcinomas. Hum Pathol 2004;35:122–8.

10. Basak S, Speicher D, Eck S, et al. Colorectal carcinoma invasion inhibition by CO17-1A/GA733 antigen and its murine homologue. J Natl Cancer Inst 1998; 90:691–7.

11. Herlyn M, Steplewski Z, Herlyn D, Koprowski H. Colorectal carcinoma-specific antigen: detection by means of monoclonal antibodies. Proc Natl Acad Sci U S A 1979;76:1438–42.

12. Fleuren GJ, Gorter A, Kuppen PJ, Litvinov S, Warnaar SO. Tumor heterogeneity and immunotherapy of cancer. Immunol Rev 1995;145:91–122.

13. Piyathilake CJ, Frost AR, Weiss H, Manne U, Heimburger DC, Grizzle WE. The expression of Ep-CAM (17-1A) in squamous cell cancers of the lung. Hum Pathol 2000;31:482–7.

14. Kuhn S, Koch M, Nübel T, et al. A complex of EpCAM, claudin-7, CD44 variant isoforms, and tetraspanins promotes colorectal cancer progression. Mol Cancer Res 2007;5:553–67.

15. Ponti D, Zaffaroni N, Capelli C, et al. Breast cancer stem cells: an overview. Eur J Cancer 2006;42:1219–24.

16. O'Brien CA, Pollett A, Gallinger S, et al. A human colon cancer cell capable of initiating tumour growth in immunodeficient mice. Nature 2007;445:106–10.

17. Ricci-Vitiani L, Lombardi DG, Pilozzi E, et al. Identification and expansion of human colon-cancer-initiating cells. Nature 2007;445:111–5.

18. Dalerba P, Dylla SJ, Park IK, et al. Phenotypic characterization of human colorectal cancer stem cells. Proc Natl Acad Sci U S A 2007;104:10158–63.

19. Li C, Heidt DG, Dalerba P, et al. Identification of pancreatic cancer stem cells. Cancer Res 2007;67:1030–7.

20. Chong JM, Speicher DW. Determination of disulfide bond assignments and N-glycosylation sites of the human gastrointestinal carcinoma antigen GA733-2 (CO17-1A, EGP, KS1-4, KSA, and Ep-CAM). J Biol Chem 2001;276:5804–13.

21. Trebak M, Begg GE, Chong JM, et al. Oligomeric state of the colon carcinoma-associated glycoprotein GA733-2 (Ep-CAM/EGP40) and its role in GA733-mediated homotypic cell-cell adhesion. J Biol Chem 2001;276:2299–309.

22. Balzar M, Briaire-de Bruijn IH, Rees-Bakker HA, et al. Epidermal growth factor-like repeats mediate lateral and reciprocal interactions of Ep-CAM molecules in homophilic adhesions. Mol Cell Biol 2001;21:2570–80.

23. Behrens J. Cell contacts, differentiation, and invasiveness of epithelial cells. Invasion Metastasis 1994;14:61–70.

24. Winter MJ, Nagelkerken B, Mertens AE, et al. Expression of Ep-CAM shifts the state of cadherin-mediated adhesions from strong to weak. Exp Cell Res 2003; 285:50–8.

25. Hashida H, Takabayashi A, Tokuhara T, et al. Clinical significance of transmembrane 4 superfamily in colon cancer. Br J Cancer 2003;89:158–67.

26. Mayer B, Klement G, Kaneko M, et al. Multicellular gastric cancer spheroids recapitulate growth pattern and differentiation phenotype of human gastric carcinomas. Gastroenterology 2001;121:839–52.

27. Guillemot JC, Naspetti M, Malergue F, et al. Ep-CAM transfection in thymic epithelial cell lines triggers the formation of dynamic actin-rich protrusions involved in the organization of epithelial cell layers. Histochem Cell Biol 2001; 116:371–8.

28. Osta WA, Chen Y, Mikhitarian K, et al. EpCAM is overexpressed in breast cancer and is a potential target for breast cancer gene therapy. Cancer Res 2004; 64:5818–24.

29. Hussain S, Pluckthun A, Allen TM, et al. Chemosensitization of carcinoma cells using epithelial cell adhesion molecule-targeted liposomal antisense against bcl-2/bcl-xL. Mol Cancer Ther 2006;5:3170–80.

30. Münz M, Kieu C, Mack B, et al. The carcinoma-associated antigen EpCAM up-regulates c-myc and induces cell proliferation. Oncogene 2004;23:5748–58.

31. Baeuerle PA, Gires O. EpCAM (CD326) finding its role in cancer. Br J Cancer 2007;96:417–23.

32. Würfel J, Rösel M, Seiter S, et al. Metastasis-association of the rat ortholog of the human epithelial glycoprotein antigen EGP314. Oncogene 1999;18:2323–34.

33. Schmidt DS, Schnölzer M, Klingbeil P, Zöller M. CD44 variant isoforms associate with tetraspanins and selectively with EpCAM: consequences on cell cell and cell matrix adhesion. Exp Cell Res 2004;297:329–47.

34. Ladwein M, Schmidt DS, Schnölzer M, et al. The cell-cell adhesion molecule EpCAM associates with the tight junction protein claudin 7. Exp Cell Res 2005; 309:345–57.

35. Le Naour F, Zöller M. EpCAM, tetraspanins and claudin-7. Front Bioscience 2008;13:5847–65.

36. Levy S, Shoham T. The tetraspanin web modulates immune-signalling complexes. Nat Rev Immunol 2005;5:136–48.

37. Hemler ME. Tetraspanin functions and associated microdomains. Nat Rev Mol Cell Biol 2005;6:801–11.

38. Kleiger G, Grothe R, Mallick P, Eisenberg D. GXXXG and AXXXA: common α-helical interaction motifs in proteins, particularly in extremophiles. Biochemistry 2002;41:5990–7.

39. Litvinov SV, Balzar M, Winter MJ, et al. Epithelial cell adhesion molecule (Ep-CAM) modulates cell-cell interactions mediated by classic cadherins. J Cell Biol 1997;139:1337–48.

40. Yovchev MI, Grozdanov PN, Zhou H, Racherla H, Guha C, Dabeva MD. Identification of adult hepatic progenitor cells capable of repopulating injured rat liver. Hepatology 2007;47:636–47.

41. Schneider D, Engelman DM. Motifs of two small residues can assist but are not sufficient to mediate transmembrane helix interactions. J Mol Biol 2004;343: 799–804.

42. Zöller M. Gastrointestinal tumors, metastasis and tetraspanins. Z Gastroenterol 2006;44:573–86.

43. Matter K, Balda MS. Epithelial tight junctions, gene expression and nucleo-junctional interplay. J Cell Sci 2007;120:1505–11.

44. Sears HJ, Atkinson B, Mattis J, et al. Phase-I clinical trial of monoclonal antibody in treatment of gastrointestinal tumours. Lancet 1982;1:762–5.

45. Riethmüller G, Schneider-Gadicke E, Schlimok G, et al.; German Cancer Aid 17-1A Study Group. Randomised trial of monoclonal antibody for adjuvant therapy of resected Dukes' C colorectal carcinoma. Lancet 1994;343:1177–83.

46. Schweizer C, Strauss G, Lindner M, Marme A, Deo YM, Moldenhauer G. Efficient carcinoma cell killing by activated polymorphonuclear neutrophils targeted with an Ep-CAMxCD64 (HEA125x197) bispecific antibody. Cancer Immunol Immunother 2002;51:621–9.

47. Sebastian M, Passlick B, Friccius-Quecke H, et al. Treatment of non-small cell lung cancer patients with the trifunctional monoclonal antibody catumaxomab (anti-EpCAM x anti-CD3): a phase I study. Cancer Immunol Immunother 2007; 56:1637–44.

48. Kirman I, Whelan RL. Drug evaluation: adecatumumab, an engineered human anti-EpCAM antibody. Curr Opin Mol Ther 2007;9:190–6.

49. Stish BJ, Chen H, Shu Y, Panoskaltsis-Mortari A, Vallera DA. Increasing anticarcinoma activity of an anti-erbB2 recombinant immunotoxin by the addition of an anti-EpCAM sFv. Clin Cancer Res 2007;13:3058–67.

50. Zeidler R, Mysliwietz J, Csánady M, et al. The Fc-region of a new class of intact bispecific antibody mediates activation of accessory cells and NK cells and induces direct phagocytosis of tumour cells. Br J Cancer 2000;83:261–6.

51. Osada M, Ito E, Fermin HA, et al. The Wnt signaling antagonist Kremen1 is required for development of thymic architecture. Clin Dev Immunol 2006;13: 299–319.

52. Nelson AJ, Dunn RJ, Peach R, Aruffo A, Farr AG. The murine homolog of human Ep-CAM, a homotypic adhesion molecule, is expressed by thymocytes and thymic epithelial cells. Eur J Immunol 1996;26:401–8.

53. Claas C, Herrmann K, Matzku S, Möller P, Zöller M. Developmentally regulated expression of metastasis-associated antigens in the rat. Cell Growth Differ 1996;7:663–78.

54. Guillemot JC, Naspetti M, Malergue F, Montcourrier P, Galland F, Naquet P. Ep-CAM transfection in thymic epithelial cell lines triggers the formation of dynamic actin-rich protrusions involved in the organization of epithelial cell layers. Histochem Cell Biol 2001;116:371–8.

55. Kallergi G, Mavroudis D, Georgoulias V, Stournaras C. Phosphorylation of FAK, PI-3K, and impaired actin organization in CK-positive micrometastatic breast cancer cells. Mol Med 2007;13:79–88.

56. Hedrick SM. T cell development: bottoms-up. Immunity 2002;16:619–22.

57. Matzku S, Komitowski D, Mildenberger M, Zöller M. Characterization of BSp73, a spontaneous rat tumor and its *in vivo* selected variants showing different metastasizing capacities. Invasion Metastasis 1983;3:109–23.

58. Cannon SC, Strittmatter SM. Functional expression of sodium channel mutations identified in families with periodic paralysis. Neuron 1993;10: 317–26.

59. Matzku S, Wenzel A, Liu S, Zöller M. Antigenic differences between metastatic and nonmetastatic BSp73 rat tumor variants characterized by monoclonal antibodies. Cancer Res 1989;49:1294–9.

60. Pape UF, Hofmann I, Langbein L, et al. Claudins form homo- and heterooligomeric complexes in tight junctions *in vivo*. Cell Struct Funct 2004;29: 1–139.